Modeling Catalytic Gauze Reactors: HCN Synthesis

The performance of the industrial HCN synthesis Andrussow reactor on a Pt gauze catalyst is simulated using rate equations for 13 simultaneous unimolecular and bimolecular surface reactions. Individual rates have been determined experimentally for reactants, intermediates, and products on polycrystalline Pt, and the model therefore contains no adjustable parameters except for reactant flux limits. Predicted selectivities of HCN formation agree quite well with those observed in commercial reactors, and a distinct optimum with feed composition is obtained near that observed experimentally. In addition, behaviors are predicted at compositions, pressures, and temperatures inaccessible to the commercial reactors. Both isothermal and nonisothermal situations are examined. Questions concerning the validity of models, reactant flux limits, and the decoupling of simultaneous surface reactions are considered.

N. Waletzko, L. D. Schmidt
Department of Chemical Engineering
and Materials Science
University of Minnesota
Minneapolis, MN 55455

Introduction

The simulation of the performance of industrial catalytic reactors using surface reaction rate expressions obtained under well-defined conditions has seldom been successful. The major problems in this task are:

1. The heat and mass flow patterns are complex in most reactors
2. Catalyst geometries are not well characterized for supported catalysts
3. Reaction rate expressions are seldom available over sufficient ranges of variables to justify extrapolation to reaction conditions
4. Most catalyst surfaces are sufficiently altered by the reactor operating environment that rates measured under reaction-controlled conditions have little relevance

Perhaps one of the simplest types of catalytic reactors to model is the gauze catalyst, used commercially in HNO_3 synthesis from NH_3 oxidation (the Ostwald process) and in HCN synthesis from CH_4, NH_3, and O_2 (the Andrussow process) (Satterfield, 1980). The commercial catalyst is a gauze 3 mm thick and up to several meters in diameter consisting of 10–50 layers of woven Pt-10% Rh gauze operated at 1,100 K (NH_3 oxidation) or 1,400 K (HCN synthesis). The HCN reaction has the stoichiometry

$$NH_3 + CH_4 + \tfrac{3}{2}O_2 \rightarrow HCN + 3H_2O$$

although many bimolecular and unimolecular reaction steps are occurring in the reactor, the least desired being NH_3 decomposition or oxidation to form N_2. The reactor length l is thus a few millimeters, and the residence time (l/v) over the catalyst is a few milliseconds.

Simplifying conditions of these reaction systems are:

1. The catalyst is self-supported metal wires rather than supported particles
2. The reactions are relatively simple ones between small polyatomic molecules whose kinetics have been studied under well-defined conditions
3. The temperature is sufficiently high that the surface has low coverages of most adsorbed species and may be self-cleaning.

In typical industrial Andrussow reactors CH_4, NH_3, and air preheated to ~100°C in an approximate 1:1:1.3 ratio of CH_4:NH_3:O_2 are passed over the reactor at a pressure somewhat above 1 atm. At this composition reaction heat produces a gauze temperature of ~1,100°C. Yields of HCN are typically 60–70% based on NH_3 converted, with N_2 and H_2O and CO being major products. Only traces of NO, CO_2, and other compounds of carbon and nitrogen are reported. The gauze temperature is usually

Correspondence concerning this paper should be addressed to L. D. Schmidt.

regarded as uniform although variations of as much as 200°C have been suggested.

Another reactor type for production of HCN is the tube wall reactor (Koberstein, 1973) developed by the Degussa Company. In this process the Pt catalyst is deposited on the wall of ceramic tubes which act as heat exchangers with the strongly endothermic reaction

$$CH_4 + NH_3 \rightarrow HCN + 3H_2$$

outside balanced by the exothermic oxidation of methane

$$CH_4 + 2O_2 \rightarrow 2H_2O + CO_2$$

inside to attain the ~1,500 K necessary to achieve ~90% yield of HCN from NH_3. As in the Andrussow process, NH_3 loss to N_2 is the major undesired reaction. The Degussa process appears to be seldom used commercially in spite of its higher yield because of materials problems in the tube wall reactor.

Catalytic combustion in tube wall reactors has been modeled extensively although usually for only one reaction. These situations have been reviewed recently (Trimm, 1983; Pfefferle and Pfefferle, 1987).

In this paper we simulate the performance of the Andrussow reactor. An essential feature of this paper is that all rate expressions (Table 1) that we use have been obtained in this laboratory on clean polycrystalline Pt at low pressures where no mass transfer limitations exist. The model therefore contains no adjustable parameters, and the calculation can therefore be regarded as a first-principles computation of the performance of these reactors. The major issues addressed are the predictions of the model and, equally important, the validity of a simple model for gauze reactors.

Model

Figure 1 shows sketches of the reactors and predicted variations of parameters as a function of position in the reactors. The gauze reactor has ~0.2 mm spaces between sheets of woven gauze wires through which gases pass down the 2–5 mm length of the gauze pack. Gases are preheated to ~100°C, and the reaction exothermicity heats the gauze to ~1,100°C. A ceramic blanket above and below the gauze distributes flow and acts as a radiation shield to keep the gauze adiabatic and at a nearly uniform temperature.

The path through the gauze is extremely tortuous, but it seems reasonable to approximate it as a tube wall reactor with reactor tube diameter d and length l, which correspond roughly to the gauze spacing and bed thickness, respectively. Gas flow is turbulent, and gases are further mixed by the path tortuosity.

We therefore model the reactor as a plug-flow tubular reactor with reactions on the wall. Some axial mixing must occur, but this should not alter the performance significantly from the plug flow assumption. An alternate model of the gauze pack is a series of mixed reactors in which each "reactor" is roughly the region between gauze layers. It can easily be shown that 10–50 mixed reactors (the typical number of gauze layers) in series yield nearly the same performance as a single unmixed reactor of the same total residence time.

We therefore use the mass and energy balance equations

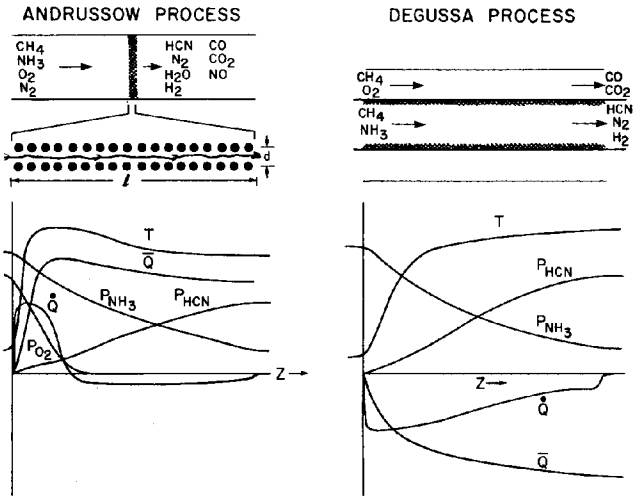

Figure 1. Reactor geometries.

a. Andrussow (gauze) process
b. Degussa (tube wall) process
Flow pattern in both is modeled as plug flow; z represents position in reactor
Heat generation curve $\dot{Q}$ is positive (heat generated) when O_2 is present, negative (heat absorbed) when O_2 has been consumed

$$v\frac{dc_j}{dz} = \frac{A}{N_o V}\sum_{i=1}^{R}\nu_{ij}r_i, \quad j = 1, 2, \ldots, S \tag{1}$$

and

$$v\rho C\frac{dT}{dz} = -\frac{A}{N_o V}\sum_{i=1}^{R}\Delta H_i r_i + h\nabla^2 T \tag{2}$$

where c_j is the concentration of species j (total S), v is the average gas velocity in the gauze, z is the position, A/V is the catalyst surface to gas volume ratio of the gauze, and r_i is the rate of the ith reaction (total R), which has a heat of reaction ΔH_i. The gas has density ρ and specific heat C, and the effective heat transfer coefficient through the gauze is h. Written in terms of partial pressures in torr with r_i in molecules/cm^2 · s we obtain

$$\frac{dP_j}{dz} = \frac{RT}{N_o v}\frac{A}{V}\sum_{i=1}^{R}\nu_{ij}r_i, \quad j = 1, 2, \ldots, S \tag{3}$$

and

$$\frac{dT}{dz} = \frac{1}{N_o v\rho C}\frac{A}{V}\sum_{i=1}^{R}\Delta H_i r_i + \frac{h}{v\rho C}\nabla^2 T \tag{4}$$

The problem is therefore that of finding P_j and T for given geometry, feed conditions, and feed velocity.

If the reactor is adiabatic and has a high heat conduction ($h\nabla^2 T$ large), the equations can be written

$$\frac{dP_j}{dt} = \sum_{i=1}^{R}\nu_{ij}r_i \quad j = 1, 2, , \ldots, S \tag{5}$$

and

$$T = T_o + \frac{1}{RT\rho C}\sum_{i=1}^{R}\Delta H_i\int_0^{\tau} r_i\,dt \tag{6}$$

where we have defined a new time variable

$$t = \frac{RT}{N_o}\frac{A}{V}\frac{z}{v} = \frac{1}{K}\frac{z}{v} \tag{7}$$

to simplify units. The time t is a measure of the time spent in the reactor, and the total time τ is proportional to the total residence time. The actual time is $z/v = t/K$. The constant K is difficult to determine accurately for a gauze catalyst because geometries and v are not well known. We report results as a function of a "time" defined as $10^{20}t$ (t defined by Eq. 7) because this gave computed times between 1 and 1,000 for complete conversion in typical calculations. In a later section we estimate the actual residence time for these conversions. We note, however, that we are interested mainly in behavior at times where the conversion of reactants is nearly complete so that performance at fixed time corresponds to a fixed residence time.

The local rate of heat generation is

$$\dot{Q}(z) = \frac{1}{N_o}\frac{A}{V}\sum_{i=1}^{R}\Delta H_i r_i \tag{8}$$

with $\dot{Q}$ in energy/volume time. The total rate of heat generation per unit volume over the reactor is

$$\bar{Q} = \frac{1}{N_o\tau}\frac{A}{V}\sum_{i=1}^{R}\Delta H_i\int_0^{\tau} r_i\,dt \tag{9}$$

In modeling we include the temperature dependences of ΔH_i but generally exclude the composition and temperature dependences of C. The latter should be a good approximation in air processes because of a large N_2 diluent. We also do not account explicitly for the temperature dependence of the gas density ρ or the change in total number of moles during reaction. These effects should be small since the temperature within the gauze is nearly uniform, and results could be corrected easily by adjusting v appropriately in comparing calculated results with performance of a particular reactor.

Sketched in Figure 1a are plots of P_{NH_3}, P_{HCN}, P_{O_2}, $\dot{Q}$, and $\bar{Q}$ expected for the Andrussow reactor. The reactant gases are heated very quickly in the gauze. In the presence of O_2, the strongly exothermic oxidation reactions generate heat. After the O_2 is consumed, endothermic reactions such as $CH_4 + NH_3 \rightarrow HCN + H_2$ dominate, and heat is absorbed ($\dot{Q} < 0$).

The Degussa process on a Pt-coated tube wall, shown in Figure 1b, should also have approximately a plug flow pattern, although the geometry and mixing are quite different, and the residence time is much longer. All reactions in the CH_4, NH_3 mixture are endothermic and $\dot{Q}$ and $\bar{Q}$ are therefore negative.

Rates

Surface reaction rates $r_i(P_j, T)$ are assumed known for all reactions in the model. Table 1 lists the 13 unimolecular and bimolecular reactions used for this simulation and their rate expressions. All were measured in this laboratory on polycrystalline Pt wires and foils for reactant pressures between 10^{-3} and 10 torr (0.133 and 1,333 Pa) for Pt temperatures between ~500 and ~1,500 K. All measurements were obtained in a steady state mixed-reactor geometry under reaction-controlled conditions with mass spectrometer sampling as described in detail in the references cited in the table. All rates were measured as functions of surface temperature in pure reactant gases with all gases at ~300 K. (Note that in the industrial reactor the gas and surface temperatures are nearly equal and this could cause some errors in rates predicted in the industrial reactor.) All rates were reproduced on several Pt wires, and in many reactions the surface was shown by Auger electron spectroscopy to be clean before reaction and free of contaminants after reaction. In no situations were significant contaminants or rate transients observed. Rates of unimolecular reaction are regarded as accurate to within better than a factor of ~2 and bimolecular reactions to within a factor of ~3. The accuracy of rate expressions is generally highest between 1,000 and 1,500 K, the range of the simulation.

All bimolecular reactions must approach flux-limited situations in positive-order regimes at sufficiently high total pressure because bimolecular rates scale as P^2. For unimolecular reactions the flux limit can easily be handled in the Langmuir-Hinshelwood formalism

$$r_R = \frac{k_R P_A}{1 + K_A P_A} \tag{10}$$

by writing

$$K_A = \frac{k_a}{k_d + k_R} \tag{11}$$

where k_a, k_d, and k_R are rate coefficients for adsorption, desorption, and reaction, respectively. Both k_d and k_R have Arrhenius temperature dependences (obtained from data of Table 1), but

$$k_a = \frac{s_o}{\sqrt{2\pi MRT_g}} \tag{12}$$

depends only weakly on temperature as $T_g^{-1/2}$ and any temperature dependence in the initial sticking coefficient s_o. Sticking coefficients have been measured (at lower temperature) for most of the species in Table 1, and for all except CH_4, s_o is found to be only a weak function of either gas or surface temperature.

For bimolecular reactions the rate expression including the flux limits can only be written as the solution of a quadratic equation. While this could be done, we have chosen to incorporate flux limits of both unimolecular and bimolecular reactions simply as

$$\nu_{ij} r_i \le \frac{s_i P_j}{\sqrt{2\pi MRT}} \tag{13}$$

We have written the program to determine rates from the expressions in Table 1; compare this value to flux limits of each reactant, and use the smaller of these rates in Eq. 5. This appears to be a reasonable approximation because the flux limit transforms the rate over a fairly narrow range of temperature and pressure from having Arrhenius temperature dependences and strong pressure dependences to being independent of T and first order in the limiting reactant and zero order in the other reactant.

For isothermal operation the compositions vs. time were obtained by integrating Eq. 5 for an assumed constant tempera-

Table 1. Reaction Rate Expressions

Reaction	Rate Expression	Reference
$NH_3 \rightarrow 3/2\ H_2 + 1/2\ N_2$	$\dfrac{4.9 \times 10^{18} \exp(-2{,}130/T) P_{NH_3}}{[1 + 0.044 \exp(2{,}390/T) P_{CH_4}/P_{NH_3}^{1/2}]^3}$ if $P_{CH_4} > 0$	Hasenberg & Schmidt (1985, 1986, 1987)
	$\dfrac{4.9 \times 10^{18} \exp(-2{,}130/T) P_{NH_3}}{1 + 4.35 \times 10^{-5} \exp(8{,}400/T) P_{NH_3} + 9.85 \times 10^{-6} \exp(13{,}850/T) P_{H_2}^{3/2}}$ if $P_{CH_4} = 0$	Loffler & Schmidt (1986)
$NH_3 + CH_4 \rightarrow HCN + 3H_2$	$\dfrac{7.80 \times 10^{18} \exp(-1{,}950/T) P_{CH_4} P_{NH_3}^{1/2}}{[1 + 0.044 \exp(2{,}390/T) P_{CH_4}/P_{NH_3}^{1/2}]^4}$	Hasenberg & Schmidt (1985, 1986, 1987)
$NH_3 + 5/4\ O_2 \rightarrow NO + 3/2\ H_2O$	$\dfrac{2.1 \times 10^{16} \exp(10{,}850/T) P_{NH_3} P_{O_2}^{1/2}}{1 + 4.0 \times 10^{-5} \exp(12{,}750/T) P_{NH_3}}$	Pignet & Schmidt (1974, 1975) Hasenberg & Schmidt (1985, 1986, 1987)
$NH_3 + 3/2\ NO \rightarrow 5/4\ N_2 + 3/2\ H_2O$	$\dfrac{1.48 \times 10^{17} \exp(3{,}875/T) P_{NO} P_{NH_3}^{1/2}}{[1 + 5 \times 10^{-5} \exp(7{,}950/T) P_{NO} + 0.0145 \exp(2{,}880/T) P_{NH_3}^{1/2}]^2}$	Takoudis & Schmidt (1983)
$1/2\ O_2 + H_2 \rightarrow H_2O$	$1.5 \times 10^{19} P_{O_2} P_{H_2}$	Blieszner (1979)
$CH_4 + 3/2\ O_2 \rightarrow CO + 2\ H_2O$	$\dfrac{4 \times 10^{19} \exp(-5{,}000/T) P_{CH_4} P_{O_2}^{1/2}}{1 + 5 \times 10^{-10} \exp(15{,}000/T) P_{CH_4}}$	Hasenberg & Schmidt (1985, 1986, 1987)
$NO + H_2 \rightarrow 1/2\ N_2 + H_2O$	$\dfrac{3.5 \times 10^{18} \exp(7{,}300/T) P_{H_2} P_{NO}}{[1 + 2.7 \times 10^{-4} \exp(9{,}750/T) P_{NO} + 15 \exp(1{,}100/T) P_{H_2}^{0.7}]^2}$	Papapolymerou & Schmidt (1985)
$NO \rightarrow 1/2\ N_2 + 1/2\ O_2$	$\dfrac{5.53 \times 10^{16} \exp(-2{,}625/T) P_{NO}}{1 + 6.95 \times 10^{-4} \exp(4{,}125/T) P_{NO} + 1.56 \exp(4{,}775/T) P_{O_2}}$	Mummey & Schmidt (1981)
$NO + CO \rightarrow 1/2\ N_2 + CO_2$	$\dfrac{3.5 \times 10^{17} \exp(2{,}900/T) P_{NO}}{1 + 4 \times 10^{-9} \exp(15{,}000/T) P_{CO}}$	Klein et al. (1985)
$CO + 1/2\ O_2 \rightarrow CO_2$	$\dfrac{2.5 \times 10^{15} \exp(16{,}000/T) P_{CO} P_{O_2}}{[3 \times 10^{-7} \exp(15{,}000/T) P_{CO} + 300 \exp(6{,}000/T) P_{O_2}]^2}$	Blieszner (1979), Schwartz et al. (1986)
$CH_4 + NO \rightarrow HCN + 1/2\ H_2 + H_2O$	$\dfrac{1.8 \times 10^{20} \exp(5{,}000/T) P_{CH_4} P_{NO}}{1 + 5 \times 10^{-10} \exp(15{,}000/T) P_{CH_4}}$	Hasenberg & Schmidt (1985, 1986, 1987)
$CO + H_2O \rightarrow CO_2 + H_2$	$\dfrac{3.65 \times 10^{17} \exp(-1{,}595/T) P_{CO} P_{H_2O}^{1/2}}{[1 + 0.048 \exp(3{,}037/T) P_{CO}]^2}$	Blieszner (1979)
$CH_4 + 3NO \rightarrow 3/2\ N_2 + CO + H_2O$	$\dfrac{1.25 \times 10^{15} \exp(5{,}000/T) P_{CH_4} P_{NO} + 3 \times 10^{20} \exp(-750/T) P_{NO} P_{CH_4}^{1/2}}{1 + 1 \times 10^{-11} \exp(20{,}000/T) P_{CH_4}}$	Hasenberg & Schmidt (1985, 1986, 1987)

ture T for particular initial P_{NH_3}, P_{CH_4}, P_{O_2}, and P_{N_2}. The total rate of heat generation was computed from Eq. 9 using calculated heats of reaction at the reactor temperature.

The total rate of heat generation depends on the reactor residence time τ. The adiabatic reactor temperature can then be obtained for any particular τ from Eq. 6.

Note that catalyst geometry factors are all grouped into K from Eq. 7. None of these is known accurately. However, by choosing a value of t where the reactant conversion is a specified value, the composition and temperature at that point can be calculated. At any other feed composition the product composition can then be calculated at that value of t which corresponds to a fixed flow situation. In other situations we are interested in a specified conversion of a reactant for different flow conditions. For these compositions, values of t are chosen for that reactant conversion. This would correspond to variation of the flow velocity v in a reactor of length l to achieve a fixed reactant conversion.

For computation of adiabatic gauze temperatures Eqs. 5 and 6 must be solved simultaneously for a particular T. This was done by computing the composition at an assumed temperature, computing T from Eq. 6 from $\bar{Q}$ obtained for a particular t, Eq. 8, and then integrating Eq. 5 successively until the temperature was found.

Calculations

HCN formation at 1,400 K

The optimum feed composition of CH_4:NH_3:O_2 in industrial reactors is approximately 1:1:1.3, the total pressure is ~2 atm, and the typical operating temperature is 1,400 K.

For the first series of simulations we used a nominal feed composition of P_{CH_4} = 200 torr (26.6 kPa), P_{NH_3} = 200 torr, and P_{O_2} = 250 torr (33.25 kPa) to give a total pressure of 1,600 torr (212.8 kPa) assuming O_2 as air (P_{N_2} = 950 torr [126.4 kPa]). We then varied the ratios of two components, keeping the third component fixed. By varying compositions we were searching for optima in feed partial pressures to yield the maximum selectivity or yield of NH_3 conversion to HCN defined from a nitrogen

balance as

$$\frac{P_{HCN}}{\Delta P_{NH_3}} = \frac{P_{HCN}}{P_{HCN} + 2\Delta P_{N_2} + P_{NO}} \tag{14}$$

for specified values of NH_3 conversion or flow conditions (time t).

In an operating reactor the total flow rate is to be maintained constant while the gas composition is varied, and this would correspond to operation at fixed t. Alternatively one might vary the flow rate of one species while keeping the other two constant, but the assumption of constant t is a reasonable approximation to this experiment for small variations in feed ratios.

Figure 2 shows a typical plot of partial pressures vs. time for the nominal feed composition listed above at 1,400 K. It is evident that P_{O_2} falls to zero by $t = 12$. It is also evident that the production of oxidation products (CO, CO_2, N_2, H_2O, and NO) essentially ceases as soon as O_2 disappears. HCN production then continues steadily until all CH_4 or NH_3 is consumed. Nitrogen production rises slowly after all O_2 is consumed and H_2 becomes the other major product.

The differential and total rates of heat generation, $\dot{Q}$ and $\bar{Q}$, are also plotted in Figure 2. $\bar{Q}$ exhibits a maximum at $t = 12$, corresponding to $\dot{Q}$ crossing zero.

Figure 3 shows a plot of HCN conversion vs. P_{CH_4}/P_{O_2} for $P_{NH_3} = 200$ torr (26.6 kPa). Figure 3a is for fixed t (flow rate) while Figure 3b is for fixed NH_3 conversion from 50 to 99%. It is evident that there is a distinct maximum at fixed flow rate and that the maximum shifts to lower P_{CH_4}/P_{O_2} as the flow rate decreases. No maximum occurs for fixed NH_3 conversion, Figure 3b, as the conversion increases monotonically with increasing P_{CH_4}. However, the conversion exhibits a distinct break such that above a certain P_{CH_4}/O_2 the rate is nearly independent of this ratio as the reaction goes to completion.

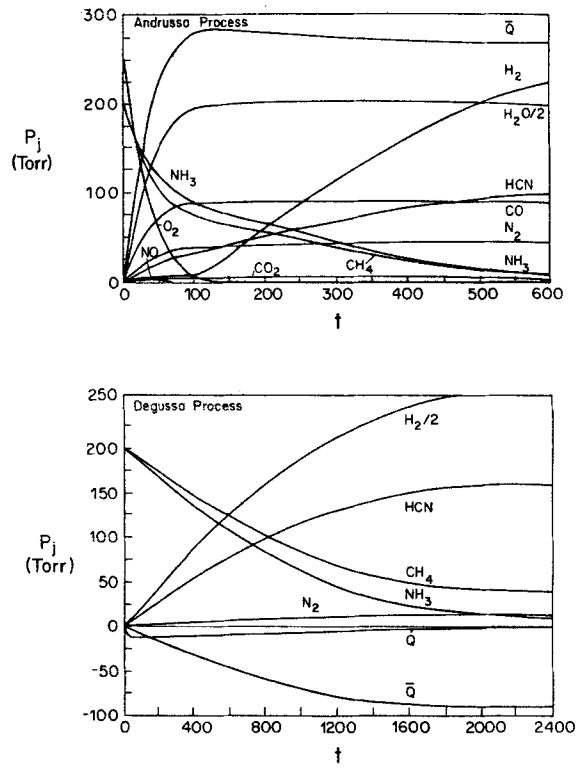

Figure 2. Species partial pressures vs. time.
Initial compositions: $P_{NH_3} = P_{CH_4} = 200$ torr, $P_{O_2} = 750$ torr, at 1,400 K
Results obtained by solving Eq. 5 with time t defined by Eq. 7

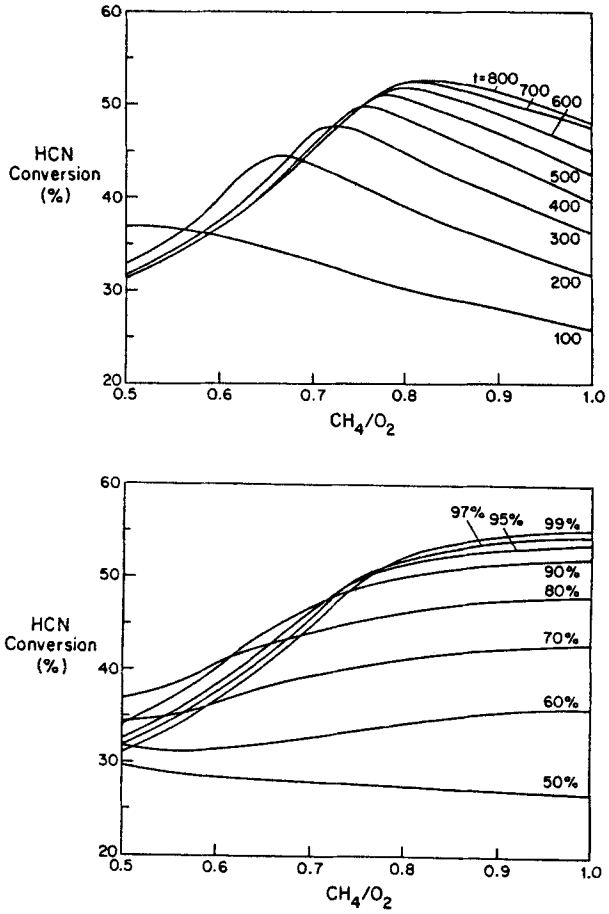

Figure 3. HCN conversion vs. initial P_{CH_4}/P_{O_2} ratio.
Fixed $P_{NH_3} = 200$ torr at 1,400 K
a. Fixed time t or flow rate
b. Fixed NH_3 conversion
A distinct maximum in conversion occurs at fixed t

The maximum for fixed flow rate occurs because, while HCN formation increases with P_{CH_4}, NH_3 is oxidized to N_2 in excess N_2 so that an optimum exists between $P_{CH_4}/P_{O_2} = 0.6$ to 0.8 depending on the flow rate chosen.

Figure 4 shows HCN production vs. variations in P_{NH_3}/P_{O_2}. It is seen that maxima also occur with P_{NH_3}/P_{O_2} variation for both constant flow rate and constant NH_3 conversion, although these are quite broad and the HCN conversion is fairly insensitive to the P_{NH_3}/P_{O_2} ratio between 0.9 and 1.2.

Figure 5 shows plots of HCN conversion vs. P_{CH_4}/P_{NH_3}. Maxima are observed at fixed flow rate and at fixed NH_3 conversion, although the maximum is sharp for fixed flow rate but very broad for fixed conversion.

Effect of temperature and total pressure

For these calculations we used $P_{CH_4} = 200$ torr (26.6 kPa), $P_{NH_3} = 200$ torr, and $P_{O_2} = 250$ torr (33.25 kPa), and varied T. Figure 6 shows plots of HCN selectivity vs. temperature for specified values of flow rate and NH_3 conversion. It is seen that the selectivity monotonically increases with increasing tempera-

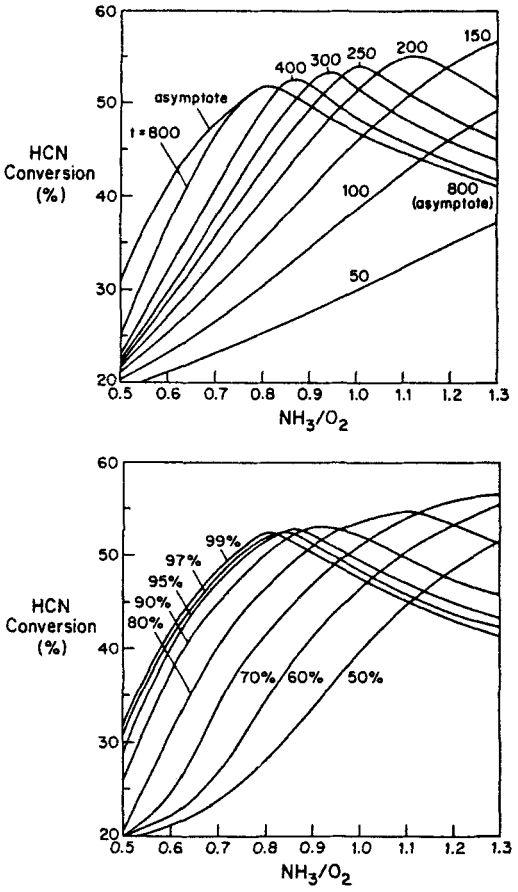

Figure 4. HCN conversion vs. initial P_{NH_3}/P_{O_2}.
Fixed P_{O_2} = 250 torr for P = 1,600 torr at 1,400 K
Maxima are observed for both fixed t and NH_3 conversion

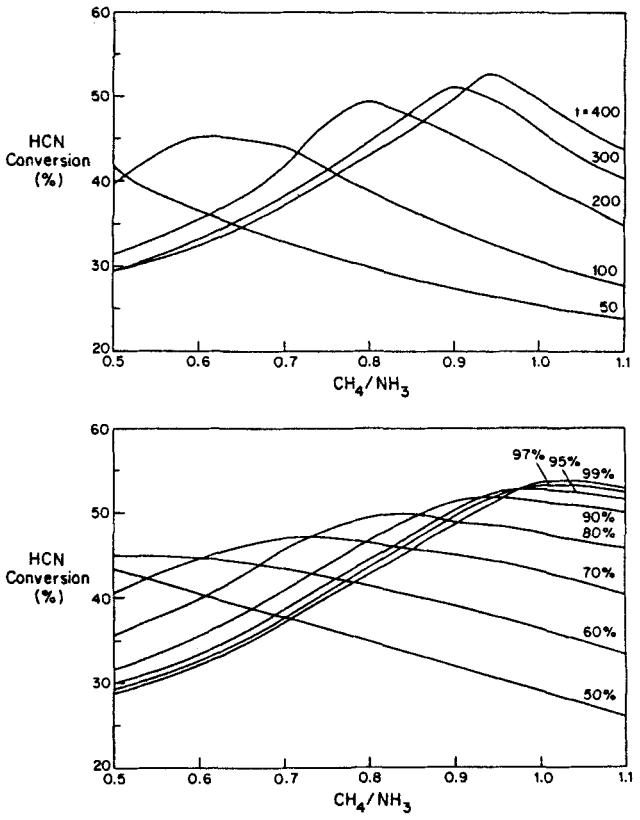

Figure 5. HCN conversion vs. initial P_{CH_4}/P_{NH_3}.
Fixed P_{O_2} = 250 torr for P = 1,600 torr at 1,400 K
Maxima are observed for both fixed t and NH_3 conversion.

ture for both constant t and conversion. The variation at fixed t is fairly large because all rates increase with t and the NH_3 conversion therefore increases. At fixed NH_3 conversion the HCN conversion is not such a strong function of T.

We also examined the effect of varying total pressure for fixed composition (1:1:1.25) at 1,400 K. Figure 7 shows that HCN conversion is a monotonically decreasing function of P, although the variation with NH_3 conversion is only a few percent at fixed NH_3 conversion for a total pressure variation of a factor of nearly 10.

We conclude from this simulation that the Andrussow process gives the highest HCN yield at the highest temperature and the lowest pressure, although the sensitivities to T and P are fairly small. The calculations suggest that high T gives the highest selectivity and of course the shortest residence time, so that the highest operating temperature consistent with materials stability should be chosen. Low pressures give the best HCN conversions, although longer residence times and lower production rates would then be required. The calculations suggest that the dependence of conversion on pressure is not a determining factor in reactor design and that operation near atmospheric pressure is probably most economical.

Calculation of gauze thickness

All compositions were computed for specified residence times that were chosen to give realistic yields or reactant conversion. In this section we estimate the reactor size predicted for this conversion.

The gauze pack consists of layers of 0.0025 cm dia. woven wires spaced at 0.03 cm. If we assume these are equivalent to a cylindrical tube of 0.03 cm dia., its surface to volume ratio would be 130 cm^{-1}. The constant K in Eq. 7 is then estimated to be 2×10^{-14} torr · cm^2/molecule (0.27×10^{-14} kPa · cm^2/molecule) at 1,400 K.

If we assume that $t = 50$ is a typical time for nearly complete conversion, we obtain a residence time of 2.5×10^{-4} s. Now if the gas velocity through the gauze is 500 cm/s (feed velocity corrected to 1,400 K and void fraction of gauze) we obtain a gauze thickness $z = vt$ of $500 \times 2.5 \times 10^{-4} = 1.2$ mm, which is within a factor of 3 of the typical 3 mm thick gauze pack used industrially.

Thus we obtain a surprisingly good agreement between calculated and experimental gauze thicknesses. This is further confirmation that the model contains no seriously inaccurate assumptions. Perhaps the most serious would be our assumption of no mass transfer limitations between the reacting tube wall and the flow gas stream. A concentration drop at the wall would lower the effective reactant partial pressures at the wall and thus require a thicker gauze for a given conversion. The calculated gauze thickness in the model in fact deviates on the opposite side of that predicted with mass transfer limitations.

Adiabatic temperature

In this section we calculate the adiabatic temperature vs. CH_4/O_2 ratio to determine how HCN yield and selectivity cor-

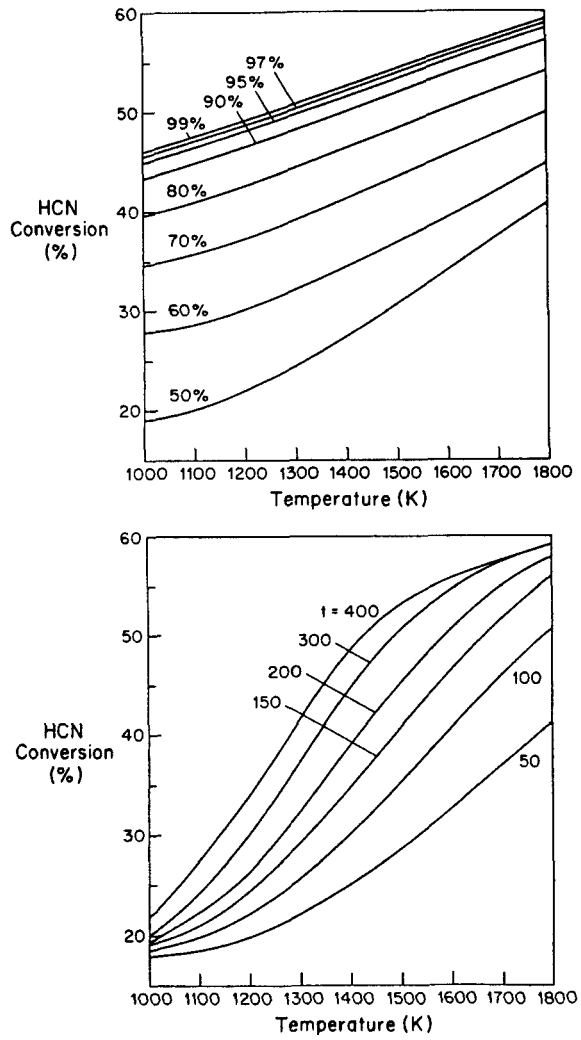

Figure 6. HCN conversion vs. reactor temperature.
Initial $P_{CH_4} = P_{NH_3} = 200$ torr, $P_{O_2} = 250$ torr (total pressure, 1,600 torr)
Rate increases monotonically with T

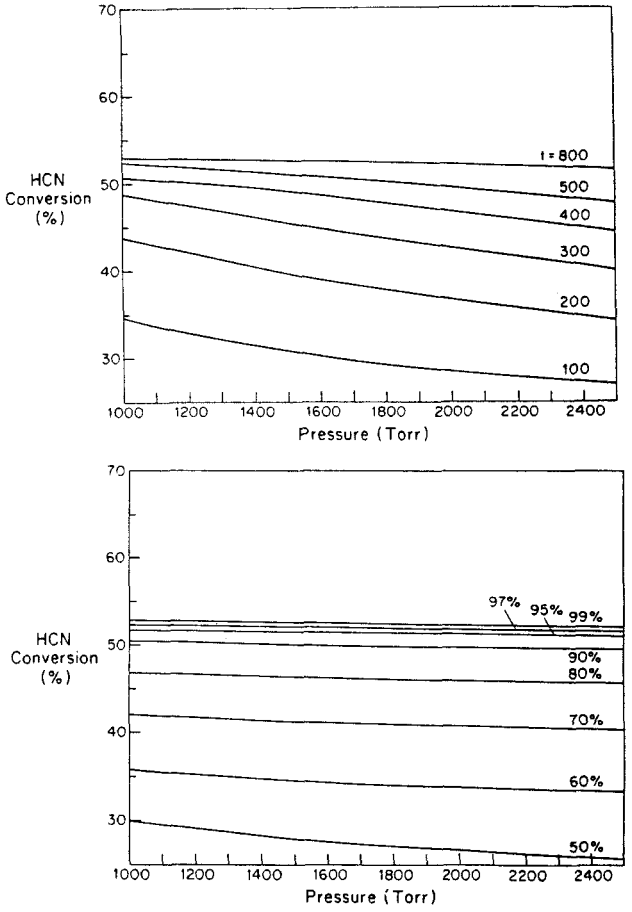

Figure 7. HCN conversion vs. total reactor pressure P.
$P_{CH_4} = P_{NH_3}$ and $P_{O_2} = 1.25\ P_{CH_4}$, at 1,400 K
Conversion is quite insensitive to P at both fixed t and NH_3 conversion

relate. Since the HCN reaction is endothermic and most others are exothermic, the minimum in gauze temperature may predict optimum operating conditions.

Figure 8 shows a plot of total heat generated, $\overline{Q}$, and the average gauze temperature, $\overline{T}$, vs. the CH_4/O_2 ratio. We emphasize that these were carried out by calculating $\overline{Q}$ assuming T = 1,400 K, and the temperature was then calculated assuming a constant heat capacity of reactant gases. This was regarded as sufficiently accurate because our interest was to explore the existence of an overall temperature minimum, and variations across the gauze would probably prevent greater accuracy.

It is seen from Figure 8 that a temperature minimum exists vs. CH_4/O_2. The exact position of the minimum shifts with residence time, going from $CH_4/O_2 = 0.75$ at $t = 300$ to lower ratios at shorter times.

One method of optimizing HCN reactor performance is to "temperature tune" by adjusting the CH_4/O_2 ratio under fixed feed and flow conditions until a minimum gauze temperature is obtained. From our calculations we find that a minimum temperature does exist and that the shift in minimum with time follows the shift in the maximum HCN conversion. However, these minima and maxima do not exactly correspond, and this does not appear to be a foolproof method to locate the optimum composition.

Nonisothermal gauze

In the previous calculations the temperature across the gauze was assumed constant at 1,400 K for variations in composition and pressure and for different temperature values at fixed composition and pressure in Figures 6 and 7.

We also calculated the temperature profile $T(z)$ expected by solving Eq. 4. The effective heat transfer coefficient in the gauze, h, is very difficult to estimate. It contains three major contributions: heat conduction through the metal contacts between gauze layers, gas conduction, and radiation. Heat conduction within the gauze depends on the area of contact between gauze layers. This depends initially on how firmly gauzes are packed, and during the course of the reaction gauze layers become tightly welded together to increase heat transfer area. This is most severe in the initial gauze layers and continues over a period of weeks to months of use of a particular gauze pack. Gas conduction depends on the heat transfer coefficient between the flowing gas and the gauze, which in turn depends on the

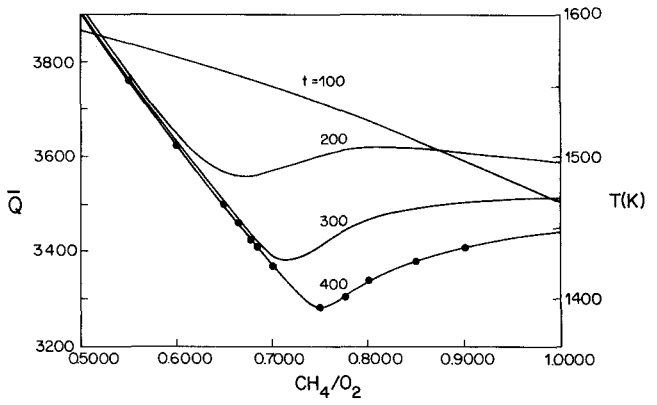

Figure 8. Total rate of heat generation $\bar{Q}$ (arbitrary units) and average temperature vs. CH_4/O_2 for indicated times.

A minimum in $\bar{Q}$ and T occurs near the maximum in HCN conversion

degree of turbulence in particular regions. In fact, the gas and surface temperatures at any position could differ. Radiative conduction could be estimated by knowing view factors of a particular gauze configuration.

We computed $T(z)$ by first determining $\dot{Q}(z)$ assuming isothermal operation and then solving

$$\dot{Q} = \alpha^{-1} \nabla^2 T \tag{15}$$

by the finite-difference method. We used 25 cells, which corresponds to the situation for a gauze pack consisting of 25 constant-temperature gauze layers. We then used $T(z)$ to calculate a new $\dot{Q}(z)$, solved Eq. 15, and iterated this procedure to convergence. Boundary conditions used were $dT/dz = 0$ on the first gauze (no upstream heat transfer) and $\bar{T} = 1{,}400$ K (gauze adiabatic).

Figure 9a shows a plot of $T(z)$ vs. z for 25 gauzes with α an adjustable parameter. It is seen that $T(z)$ is nearly a straight line except on the first few gauzes. The local rate of heat generation, $\dot{Q}$, is strongly positive only near the first few gauzes where O_2 is still present. The heat removal ($\dot{Q} < 0$) along the rest of the gauzes makes the curve convex but does not cause any dramatic deviation from linearity because $\dot{Q}$ is fairly small in the endothermic region.

Figure 9b shows a plot of HCN conversion vs. t for α values shown. A lower heat transfer coefficient (large α) gives a faster approach to maximum HCN conversion, while isothermal operation ($\alpha = 0$, lowest curve in Figure 9b) gives the slowest approach to the maximum HCN conversion. However, the ultimate HCN yield only increases by ~4% for $\alpha = 0.1$ compared to $\alpha = 0$.

We conclude from these simulations that the temperature variations of a nonisothermal gauze should produce only a slight increase in HCN selectivity because the HCN conversion is not a strong function of temperature. Adequate performance is obtained with an isothermal catalyst gauze because the exothermicity of the early oxidation reactions provides the heat necessary to sustain the temperature in HCN formation by endothermic reactions over later gauzes. A variable temperature situation is difficult to characterize and is generally undesirable

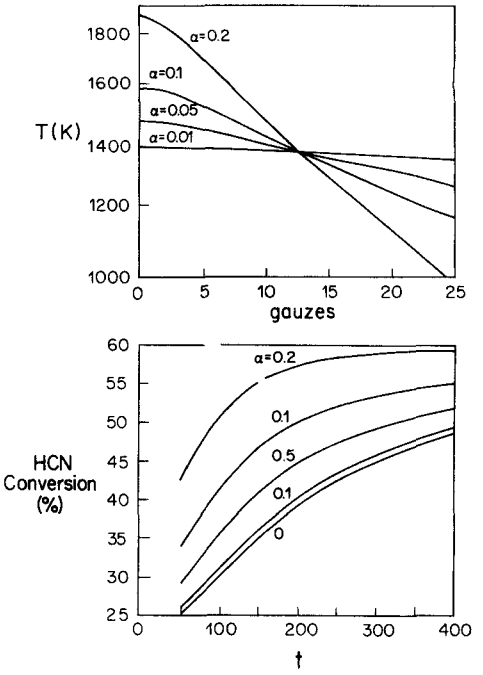

Figure 9. Calculation of T and HCN conversion for nonisothermal gauzes.

a. Calculated temperature profiles for various intergauze heat transfer coefficients α in Eq. 15

b. HCN conversions vs. time for α values shown

Isothermal operation ($\alpha = 0$) requires a longer time for complete reaction, but ultimate HCN conversions are only a few percent larger with $\alpha = 0.2$, which exceeds the melting point of the gauze or early gauzes

because of melting of early gauzes even when the average temperature appears safe.

Degussa process

It is interesting to compare these calculations with the Degussa process in which reactants are CH_4 and NH_3 only, and reaction occurs on the walls of ceramic tubes impregnated with Pt. We assume that plug flow geometry also applies to this situation, Figure 1b, although the reactors are, of course, quite different.

Results are plotted in Figure 10. It is seen that the HCN conversion is close to 85% for almost all conditions. In excess NH_3, Figure 10b, the HCN continues to fall for long times because of NH_3 decomposition. The HCN conversion increases only weakly with pressure (83% at 200 torr [26.6 kPa] and 87% at 2,000 torr [266 kPa]) for $CH_4/NH_3 = 1$ as shown in Figure 10b. The HCN conversion is also only weakly dependent on temperature (82% at 1,200 K to 87% at 1,600 K) as shown in Figure 10a.

The model predicts that the Degussa reaction is not very sensitive to T, P, or composition. Best HCN conversion is obtained at the highest temperature (limited by structural stability of the ceramics) and at high pressure. Reactant ratios near 1:1 are optimal because they yield the most complete reaction. Our maximum conversions, ~85%, are somewhat lower than reported for the industrial reaction, but, as in the Andrussow process, we did not attempt to improve yields by adjusting flux limits or other parameters in the system.

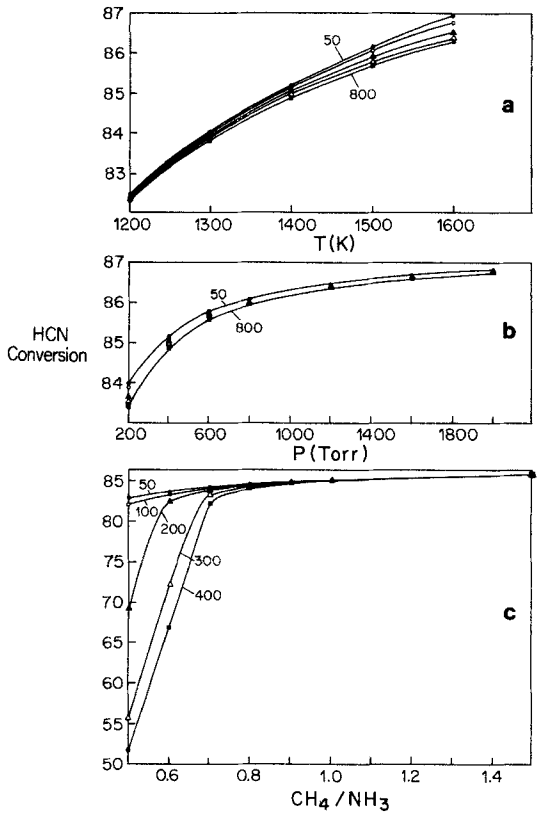

Figure 10. HCN conversion in the Degussa process, $P_{O_2} = 0$.

a. HCN conversion vs. temperature at $CH_4/NH_3 = 1$ and $P = 1$ atm

b. HCN conversion vs. total pressure for $CH_4/NH_3 = 1$ at 1,400 K

c. HCN conversion vs. P_{CH_4}/P_{NH_3} for indicated times at 1,400 K

Decoupling Surface Reactions

For homogeneous reactions in gases, any process can be rigorously decomposed into a set of unimolecular and bimolecular steps from which the composition vs. time and position can be solved using the relevant mass balance equations for a specific fluid flow situation. This is the basic assumption for modeling homogeneous reactors (in the absence of wall effects), flames, and atmospheric and other environmental situations.

For surface reactions the decoupling of processes into individual steps is in general not possible because:

1. There is an essential transport step of reactants and products between the bulk phase and the surface
2. Surface reactions usually occur at a very high density (in two dimensions) where reaction events are not necessarily independent

Therefore the model we have just examined is subject to these defects, and results are questionable if these effects are significant. We shall consider each of these in turn.

Flux and diffusion limits

Reaction occurs by gases flowing through the gauze, diffusing to the surface, adsorbing, reacting, and products desorbing and diffusing back into the flowing stream. Steady state at any position near a surface requires that

$$\Sigma\alpha_{rj}r_i = r_{aj} = k_{mj}(P_{jo} - P_j) \tag{16}$$

where the first term is the total rate of creation and loss of species j, r_{aj} is its rate of adsorption, k_{mj} is its mass transfer coefficient, and P_{jo} and P_j are the partial pressures in the flowing stream and at the surface, respectively.

As discussed previously, $\Sigma\alpha_{ij}r_i$ cannot exceed the flux to the surface, r_{aj}, Eq. 13. As long as the flux is much greater than the reaction rate, the reaction rate can be written assuming adsorption-desorption equilibrium to obtain a Langmuir-Hinshelwood (LH) rate expression $r_i(P_j, T)$, and all rate expressions listed in Table 1 were obtained under LH conditions. At sufficiently high pressures and temperatures all bimolecular rates must approach flux limits, and we have approximated this as a sharp transition that occurs whenever $\alpha_{ij}r_i = r_{aj}$ in our model, Eq. 13.

We have done this assuming a sticking coefficient S_j for each species. We have assumed $S_j = 0.1$ for all species except O_2, for which we used $S_o = 0.01$. This assumption gave reasonable results and is in qualitative agreement with sticking coefficients measured on Pt under ultrahigh vacuum conditions.

In fact, according to Eqs. 13 and 15, we should have used the sum of all reactions in determining the flux limiting condition. For example, there are six reactions in which NH_3 is a reactant, and the sum of all of these cannot exceed $10^{20}P_{NH_3}$ (rate in molecules/cm^2 · s and P_{NH_3} in torr) if $S_{NH_3} = 0.1$. One would then have to divide this NH_3 flux into all six reaction channels to decide how NH_3 is consumed. This is not possible with available information on reaction rates. To illustrate, consider bimolecular reactions of species A

$$A + B \rightarrow \text{products}, r_1 = k_1\theta_A\theta_B = \frac{k_1K_{1A}K_BP_AP_B}{(1 + K_AP_A + K_BP_B)^2} \tag{17}$$

and

$$A + C \rightarrow \text{products}, r_2 = k_2\theta_A\theta_C = \frac{k_2K_{2A}K_CP_AP_C}{(1 + K_AP_A + K_BP_C)^2} \tag{18}$$

The flux limit on A requires that

$$r_{aA} = \frac{S_AP_A}{\sqrt{2\pi M_ART}} = r_1 + r_2 = k_1K_{1A}P_AP_B + k_2K_{2A}K_BP_AP_C \tag{19}$$

because the flux limit will only occur in the regime of low coverages and positive-order kinetics. As P_A is increased, one reaction will probably approach its flux limit before the other. This will also affect the slower reaction, however, because species A is being removed by the faster reaction and thus is unable to react in the slower reaction. The ratio of these rates is

$$\frac{r_1}{r_2} = \frac{k_1\theta_B}{k_2\theta_C} = \frac{k_1K_BP_B}{k_2K_CP_C} \tag{20}$$

in *either* reaction-limited or flux-limited situations. Therefore,

one can see that the ratio depends strongly on temperature because of the Arrhenius temperature dependences of k_1, k_2, K_B, and K_C and on the partial pressures of the other reactants.

Mass transfer also limits reaction rates. The expression with mass transfer limitation has the *same functional form* as with flux limitation, namely, the rate becomes first order in the limiting species and zero order in other species in the rate expression that are in excess. The rates will also become nearly independent of temperature when mass-transfer limited. The mass transfer coefficient k_{mj} is nearly the same for all gases (except H_2) because molecular weights do not vary significantly, but values of k_m are difficult to estimate accurately because flow conditions and geometry are poorly known. However, since mass transfer rates have the same dependences on partial pressure and temperature as flux limits, both can be induced through an effective sticking coefficient. With mass transfer, this will be less than that due to flux limitation and will be nearly identical for all gases. Mass transfer coefficients are inversely proportional to total pressure, and at high pressure mass transfer limitations will become more important.

Species coupling

Another complication in decoupling surface reactions is the possible influence of a species on a reaction that does not enter directly as a reactant or product. These species are generally referred to as poisons and promoters in catalysis. As an example we showed previously (Hasenberg and Schmidt, 1987; Hwang and Schmidt, 1987) that a surface carbon or nitrile species was very strongly bound on Pt in CH_4—NH_3 mixtures and that this poisoned the Pt surface for the NH_3 decomposition reaction, which allowed HCN formation to predominate.

This can occur simply as adsorption site blocking because most species in these reactions adsorb competitively on Pt. It can also occur by surface modification in which a strongly adsorbed species chemically modifies adjacent sites to be more strongly or weakly adsorbing for another species.

Equally serious is the fact that an intermediate may react to form many different products, depending on other adsorbates. For example, carbon could react to form CO, CO_2, CH_4, and HCN depending on the presence of coadsorbed O, H, NH, etc. These products are not necessarily produced at rates predicted by the individual rate with the other reactant coming from O_2, H_2, and NH_3 individually.

A crucial assumption in an independent reactions model is the absence of significant coverages of these species, and the justification of this assumption is that most coverages are small under the reaction conditions of the HCN reactor. It can be shown that the coverage of a species is low under reaction conditions (1,400 K and 1 atm) if its heat of adsorption is less than ~60 kcal/mol. This can be done by calculating the heat of adsorption E_A necessary for one-half monolayer at 1,400 K at 200 torr (26.6 kPa; the temperature and reactant partial pressure used in the model) from the relation

$$E_A = RT \ln\left(\frac{1}{2}\frac{\nu_o\sqrt{2\pi MRT_g}}{S_oP}\right) \tag{21}$$

which gives 65 kcal/mol assuming $\nu_o = 10^{13}\text{s}^{-1}$ and $S_o = 1$. None of the adsorbates in this reaction system has a sufficiently high heat of adsorption to attain appreciable coverages under these conditions except C and CN.

We therefore conclude that it is reasonable to assume that these rates can be decoupled except for those reactions involving C or CN. These species were explicitly included in deriving rates of $CH_4 + NH_3$ and for NH_3 decomposition.

Conclusions

We have presented a "first-principles" simulation of the industrial Andrussow process in that the model contains no adjustable parameters and all rates and most sticking coefficients are experimentally measured.

The model gives a very accurate prediction of the composition optimum and a fairly accurate prediction of the optimum selectivity (low by ~10%). It also predicts production of some of the minor products to within the accuracy to which they are known. The required gauze thickness is also predicted to within approximately the accuracy to which relevant parameters are known. We suggest, therefore, that the assumptions in deriving this model are probably generally correct. This implies that:

1. The reactions and rate expressions of Table 1 are the major ones involved
2. The modeling equations are appropriate

The model should therefore be useful in simulating other operating conditions in the Andrussow process. It predicts that the reactor should operate at the highest temperature possible and that the selectivity increases only slightly with total pressure, which implies that higher pressures are desirable to increase production.

The model does not yet contain HCN hydrolysis reactions, HCN polymerization, rates of formation of other minor products such as CH_3CN, or the effects of feed impurities such as higher hydrocarbons. These could be added as these parameters become known.

We conclude that it appears to be possible to model catalytic gauze reactors fairly accurately. The most likely candidates for first-principles catalytic reactor modeling should be those operating at sufficiently high temperatures that multiple reactions can be successfully decoupled to predict multiple reaction situations from single reaction rate measurements.

Acknowledgment

This research was partially supported by the National Science Foundation, Grant No. DMR 82126729.

Literature Cited

Bliesznер, J., Ph.D. Thesis, Univ. Minnesota (1979).
Hasenberg, D., and L. D. Schmidt, "HCN Synthesis from CH_4 and NH_3 on Clean Rh," *J. Catal.*, **91**, 116 (1985).
———, "HCN Synthesis from CH_4 and NH_3 on Clean Pt," *J. Catal.*, **97**, 156 (1986).
———, "HCN from CH_4, NH_3, and O_2 on Clean Pt," *J. Catal.*, **104**, 441 (1987).
Hwang, S. Y., and L. D. Schmidt, "Decomposition of CH_3NH_2 on Pt(111)," *Surf. Sci.*, **188**, 219 (1987).
Klein, R. L., S. B. Schwartz, and L. D. Schmidt, "Kinetics of the NO and CO Reaction on Clean Pt: Steady State Rates," *J. Phys. Chem.*, **89**, 4908 (1985).
Koberstein, E., "Model Reactor Studies of HCN Synthesis from CH_4 and NH_3," *Ind. Eng. Chem. Process Des. Dev.*, **12**, 444 (1973).
Loffler, D. G., and L. D. Schmidt, "Kinetics of NH_3 Decomposition on

Polycrystalline Iron at High Temperatures, *J. Catal.*, **41,** 440 (1976).
Mummey, M. J., and L. D. Schmidt, "Decomposition of NO on Clean Pt near Atmospheric Pressures. I: Steady State Kinetics," *Surf. Sci.*, **109**(29), 43 (1981).
Papapolymerou, G. A., and L. D. Schmidt, "Unimolecular Reactions of NO, N_2O, NO_2, and NH_3 on Rh and Pt," *Langmuir*, **1,** 488 (1985).
Pfefferle, L. D., and W. C. Pfefferle, "Catalysis in Combustion," *Cat. Rev.—Sci. Eng.* **29,** 219 (1987).
Pignet, T. P., and L. D. Schmidt, "Selectivity of NH_3 Oxidation on Pt," *Chem. Eng. Sci.*, **29,** 1123 (1974).
———, "Kinetics of NH_3 Oxidation of Pt, Rh, and Pd," *J. Catal.*, **40,** 212 (1975).
Satterfield, C. N., *Heterogeneous Catalysis in Practice*, McGraw-Hill, New York, 221 (1980).
Schwartz, S. B., L. D. Schmidt, and G. B. Fisher, "The CO + O_2 Reaction on Rh(111): Kinetics and Coverages," *J. Phys. Chem.*, **90,** 6194 (1986).
Takoudis, C. G., and L. D. Schmidt, " Reaction Between NO and NH_3 on Polycrystalline Pt. I: Steady State Kinetics," *J. Phys. Chem.*, **87,** 958 (1983).
Trimm, D. L., "Catalytic Combustion," *Appl. Cat.*, **7,** 249 (1983).

Manuscript received Aug. 3, 1987, and revision received Feb. 9, 1988.